

Article

Sensitivity Analysis of Biosensors Based on a Dielectric-Modulated L-Shaped Gate Field-Effect Transistor

Chen Chong, Hongxia Liu ^{*}, Shulong Wang ^{*}, Shupeng Chen and Haiwu Xie 

Key Laboratory for Wide-Band Gap Semiconductor Materials and Devices of Education, The School of Microelectronics, Xidian University, Xi'an 710071, China; 18829029042@163.com (C.C.); chenshupeng999@126.com (S.C.); xiehaiwu.love@163.com (H.X.)

* Correspondence: hxliu@mail.xidian.edu.cn (H.L.); slwang@xidian.edu.cn (S.W.); Tel.: +86-029-88204085 (H.L.)

Abstract: Label-free biomolecular sensors have been widely studied due to their simple operation. L-shaped tunneling field-effect transistors (LTFETs) are used in biosensors due to their low subthreshold swing, off-state current, and power consumption. In a dielectric-modulated LTFET (DM-LTFET), a cavity is trenched under the gate electrode in the vertical direction and filled with biomolecules to realize the function of the sensor. A 2D simulator was utilized to study the sensitivity of a DM-LTFET sensor. The simulation results show that the current sensitivity of the proposed structure could be as high as 2321, the threshold voltage sensitivity could reach 0.4, and the subthreshold swing sensitivity could reach 0.7. This shows that the DM-LTFET sensor is suitable for a high-sensitivity, low-power-consumption sensor field.

Keywords: dielectric-modulated L-shaped tunneling field-effect transistor (DM-LTFET); biosensor; sensitivity



Citation: Chong, C.; Liu, H.; Wang, S.; Chen, S.; Xie, H. Sensitivity Analysis of Biosensors Based on a Dielectric-Modulated L-Shaped Gate Field-Effect Transistor. *Micromachines* **2021**, *12*, 19. <https://dx.doi.org/10.3390/mi12010019>

Received: 23 November 2020

Accepted: 24 December 2020

Published: 27 December 2020

Publisher's Note: MDPI stays neutral with regard to jurisdictional claims in published maps and institutional affiliations.



Copyright: © 2020 by the authors. Licensee MDPI, Basel, Switzerland. This article is an open access article distributed under the terms and conditions of the Creative Commons Attribution (CC BY) license (<https://creativecommons.org/licenses/by/4.0/>).

1. Introduction

In recent years, field-effect transistor (FET) biosensors have been studied by many researchers [1–5]. However, metal oxide semiconductor field-effect transistors (MOSFETs) cannot break through the 60 mV/dec limit due to the conduction mechanism of thermionic emission. Tunneling field-effect transistors (TFET) can make the sub-threshold swing lower than 60 mV/dec due to its band-to-band tunneling (BTBT) conduction mechanism; therefore, TFET-based sensors are increasingly attracting researchers' attention [6–10].

Dielectric modulation is used to engrave a part of the gate oxide under the gate electrode to form a nanocavity, which is then filled with biomolecules. The dielectric constant of the cavity changes (different biomolecules have different dielectric constants) and the electrical characteristics of the device also change, which is reflected in the changes in the transfer curve and sensitivity. Due to its low cost and easy operation, dielectric modulation is applied in biosensors [11–14]. Therefore, sensors made using dielectric modulation based on a TFET have been studied by many scholars [15–18]. In 2016, Kanungo et al. studied the influence of silicon germanium (SiGe) sources and n+-pocket-doped channels on dielectric modulation sensors. Studies have shown that in order to maximize the sensitivity, the proportion of germanium should be kept at 10% [19]. In 2019, through Technology Computer-Aided Design (TCAD) simulations that were used to identify the sensitivity of a double-gate dielectric modulation junctionless TFET for biomolecule recognition, Wadhwa and Raj studied the influence of the cavity length, different biomolecules, and different charges on the drain current, subthreshold swing (SS), and I_{on}/I_{off} [20]. Mohammad et al. conducted research on biosensors based on a SiGe source dual-gate TFET. The effects of cavity length, the presence or absence of biomolecules, and biomolecules with different charge concentrations on the sensitivity of the sensor were studied. However, the study did not carefully consider the influence of different biomolecules or the positive charge of the biomolecules on the sensor sensitivity [21]. In [22], Wadhwa studied the effect of

the fill factor of biomolecules on the transfer characteristics of a dual-gate junctionless TFET sensor.

However, most of the studies in the literature are based on dual-gate TFET sensors, and there are few studies on single-gate sensors. Dual-gate TFETs need cavities to be etched under both gate electrodes. In a dielectric-modulated L-shaped tunneling field-effect transistor (DM-LTFET), only one cavity needs to be etched under the gate electrode, which is then filled with biomolecules; this setup is simple to operate and low in cost. Because the source and gate overlap, the tunneling area of an LTFET is much larger than that of a planar TFET. The greater the on-state current, the better the electrical characteristics of the LTFET. Therefore, the sensitivity of a DM-LTFET is also higher. In this study, the cavity depth was deep enough, and the gate control ability was stronger.

In this study, the performance and underlying working mechanism of DM-LTFET-based biosensors were investigated. A detailed study was carried out to develop a comprehensive understanding of the working principle of the proposed biosensors and is presented as follows. Section 2 characterizes the basic device structure, simulation model, and method. Section 3 discusses the influence of different parameters on the sensitivity of a DM-LTFET biosensor. In detail, the influences of different biomolecules (different dielectric constants, different biomolecules), the cavity thickness and charged biomolecules on transfer characteristics, and the current sensitivity and threshold voltage sensitivity of the proposed sensor were studied. Section 4 concludes the paper.

2. Device Structures and Simulation Approach

A cross-sectional view of a DM-LTFET-based biosensor is shown in Figure 1. In this simulation, the source, drain, channel, and substrate material were all silicon. HfO_2 was used as the gate dielectric. In order to make the sensitivity parameter change more obvious, a gate metal work function that allowed for easier tunneling was adopted. This is why the metal work function $\Phi_{MS} = 4.2$ eV (over the HfO_2 gate oxide) was chosen. The cavity was etched under the gate electrode and filled with small biomolecules, thereby realizing the function of a dielectric modulation biosensor. The exhaustive physical and technological parameters of the structure in the DM-LTFET are shown in Table 1. In this study, six kinds of small biomolecules with different dielectric constant values (1, 2.5, 5, 11, and 23) were used to fill nanogap cavities of different thicknesses (5, 7, 9, 11, and 13 nm) and were given different amounts of charge to be studied and analyzed when the DM-LTFET was in the on-state ($V_d = 0.5$ V, $V_g = 1$ V, $V_s = 0$ V). This was mainly done by analyzing parameters such as the threshold voltage sensitivity ($S_{V_{th}}$), current sensitivity (S_{cur}), and sub-threshold swing sensitivity (S_{SS}), which can respectively be expressed as [23]:

$$S_{V_{th}} = \frac{V_{th(air)} - V_{th(bio)}}{V_{th(air)}} \quad (1)$$

$$S_{cur} = \frac{I_{on(bio)} - I_{on(air)}}{I_{on(air)}} \quad (2)$$

$$S_{SS} = \frac{SS_{air} - SS_{bio}}{SS_{air}} \quad (3)$$

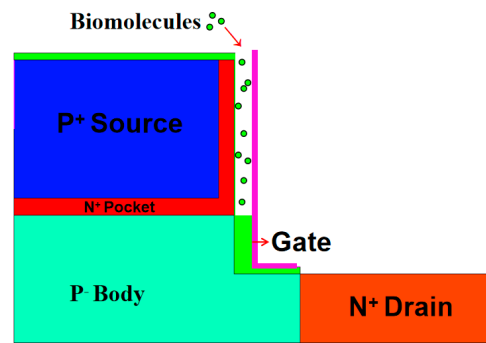


Figure 1. Schematic cross-sectional view of a dielectric-modulated L-shaped tunneling field-effect transistor (DM-LTFET) biosensor.

Table 1. Device parameters used for the simulation.

Parameter Name	Symbol	Value	Unit
Pocket thickness	T_p	5	nm
Oxide thickness	T_{ox}	2	nm
Channel doping	N_c	1×10^{15}	cm^{-3}
Source doping	N_s	1×10^{20}	cm^{-3}
Drain doping	N_d	1×10^{18}	cm^{-3}
Pocket doping	N_p	1×10^{19}	cm^{-3}
Source length	L_s	68	nm
Drain length	L_d	65	nm
Cavity height	H_c	45	nm
Gate work function	Φ_{ms}	4.2	eV

The performance of the proposed DM-LTFET biosensor was simulated using computer-aided design (Sentaurus, O-2018.06-SP2, Synopsys, Mountain View, CA, USA). In order to simulate the device parameters accurately, suitable models were selected.

The magnitude of the tunneling current has a strong dependence on the degree of band bending and the boundary profile. The nonlocal tunneling model is more consistent with the actual situation of the TFET simulation. The model considered that every point of the electric field on the tunneling path was a variable, which meant that the BTBT tunneling probability depended on the band bending at the tunneling junction. Hence, the nonlocal BTBT model was adopted in this study. The rate of the BTBT tunneling is expressed as:

$$G_{BTBT} = A \left(\frac{E}{E_0} \right)^P \exp\left(-\frac{B}{E_0}\right) \quad (4)$$

where $E_0 = 1 \text{ V/cm}$, $P = 2.5$, $A = 4 \times 10^{14} / \text{cm}^3 \cdot \text{s}$ and $B = 9.9 \times 10^6 \text{ V/cm}$ (the values of E_0 and P are default values and the values of parameters A and B are obtained through model calibration [24]).

Because the cavity was filled with small biomolecules, it was necessary to introduce the bimolecular recombination model to calibrate the recombination model in this area. The bimolecular recombination rate is given by:

$$R_{bimolec} = \gamma \cdot \frac{q}{\varepsilon_0 \varepsilon_r} \cdot (\mu_n + \mu_p) \left(np - n_{i,eff}^2 \frac{n_{se}}{n_{se}^{eq}} \right) \quad (5)$$

where γ is a prefactor for the singlet exciton; q is the elementary charge; ε_0 and ε_r denote the free space and relative permittivities, respectively; μ_n and μ_p are the electron mobility and hole mobility, respectively; n and p are the electron concentration and hole concentration, respectively; $n_{i,eff}$ is the effective intrinsic carrier concentration; n_{se} is the singlet exciton density; n_{se}^{eq} denotes the singlet-exciton equilibrium density.

3. Results and Discussion

This section mainly discusses the analysis and the simulation results. The sensitivity analysis of a sensor requires a certain comparative reference; therefore, this study used air, which filled the cavity, as a reference for discussion. The effects of five different biomolecules, seven different cavity thicknesses, and six different charged biomolecules on the sensitivity of the device were studied.

3.1. Impact of Different Biomolecules in the DM-LTFET

This section discusses the effect of filling the cavity with small biomolecules that had different dielectric constants on the sensitivity of the proposed sensor when the cavity thickness was 5 nm ($T_c = 5$ nm).

Figure 2 shows the transfer characteristic, S_{cur} , energy band variation, and $S_{V_{th}}$ of the DM-LTFET in the on-state when different biomolecules filling the cavity provided different dielectric constants. As can be seen in Figure 2a,b, as the dielectric constant increased, the on-state current (I_{on}) of the DM-LTFET increased, and S_{cur} also increased. At the same time, when the dielectric constant was greater than 10, the distance between the transfer curves of the device became smaller, and the increases in I_{on} and S_{cur} also became smaller. Figure 2c is an energy band diagram taken along the y -axis along the source, pocket, and body regions. It can be seen from Figure 2c that as the dielectric constant of the biomolecules increased, the gate control capability of the DM-LTFET became stronger, and the energy band of the body region became lower. Consequently, the probability of tunneling through the source–body junction was greater, and therefore, the greater the current collected by the drain, the greater the I_{on} and S_{cur} . At the same time, when k was greater than 10, the energy band change of the body region was also very small, which was consistent with the change in the transfer curve. Figure 2d shows that as k increased, the threshold voltage (V_{th}) of the DM-LTFET decreased and the DM-LTFET was easier to turn on. It can be seen from the energy band diagram of Figure 2c that as k increased, the more the band bent, the smaller the gate voltage required for the LTFET to reach the on state, that is, the smaller the V_{th} . At the same time, the $S_{V_{th}}$ of the sensor also improved. Simultaneously, when k was greater than 11, the band bending amplitude became smaller; therefore, the V_{th} increase was also very small when k was greater than 11. Therefore, when k was greater than 11, $S_{V_{th}}$ tended to be saturated.

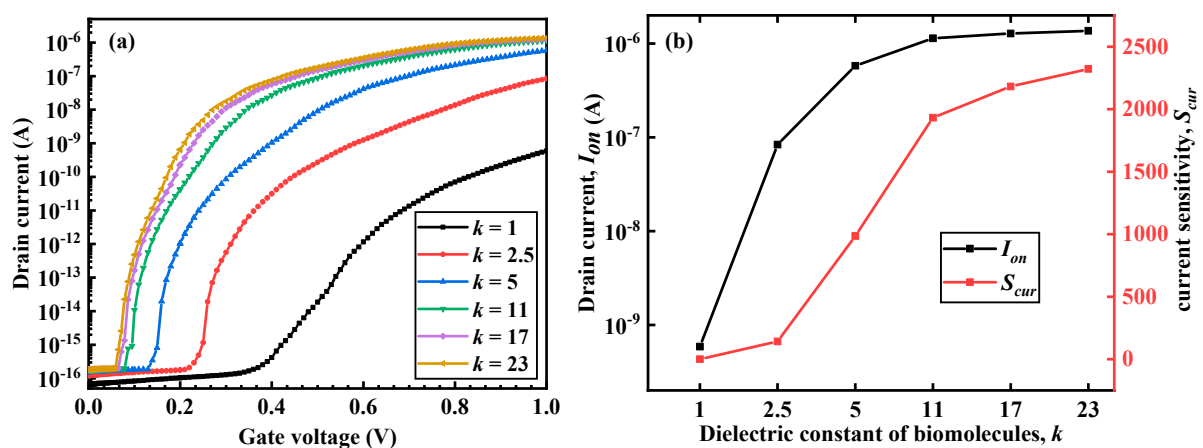


Figure 2. Cont.

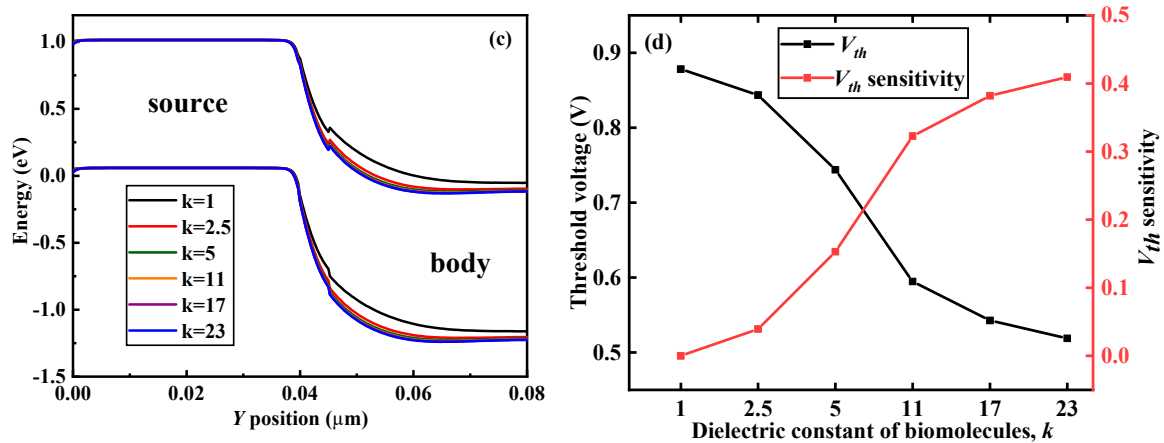


Figure 2. (a) Transfer characteristics, (b) I_{on} and S_{curr} , (c) energy band variation with respect to the y -axis, and (d) $S_{V_{th}}$ of the DM-LTFET biosensor for different values of k at $V_d = 0.5$ V, $V_g = 1$ V, and $T_c = 5$ nm.

The SS is defined as the amount of change in the gate voltage required to reduce the drain current by an order of magnitude. The SS is given by:

$$SS = \frac{dV_G}{d\Psi_S} \frac{d\Psi_S}{d(\log_{10} I_D)} \cong \left(1 + \frac{C_d}{C_{ox}}\right) \ln 10 \frac{KT}{q} \quad (6)$$

where V_G is the gate voltage, Ψ_S is the potential, I_D is the leakage current, C_d is the depletion capacitance, C_{ox} is the gate oxide layer capacitance, K is the Boltzmann constant, T is the temperature, and q is the charge. Figure 3 shows the SS–drain current characteristic curve and the change curve of S_{SS} under different k values. It can be clearly seen from Figure 3a that as k increased, the SS of the device decreased. Furthermore, the larger the k , the larger the current range where SS was lower than 60 mV/dec, and the better the performance of the DM-LTFET. As k increased, C_{ox} increased and C_d decreased (because the width of the depletion layer decreased, thus C_d decreased); therefore, SS increased. As depicted in Figure 3b, as k increased, S_{SS} also increased. Furthermore, when k was greater than 10, the S_{SS} variation range of the proposed sensor became smaller. This was due to the fact that when k was greater than 10, the width of the depletion layer reached the maximum, such that C_d changed little but C_{ox} still increased; therefore, the S_{SS} change range became smaller.

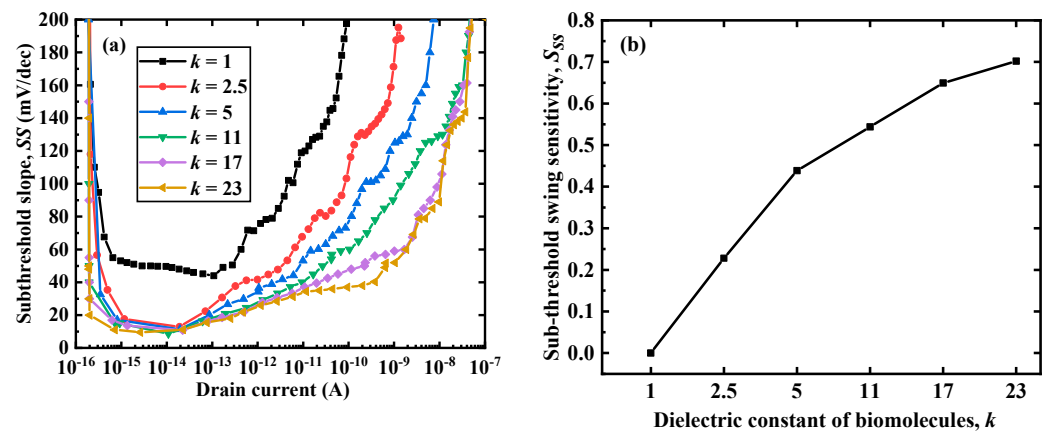


Figure 3. (a) $SS-I_d$ characteristics and (b) S_{SS} of the DM-LTFET with different biomolecules when $V_d = 0.5$ V, $T_c = 5$ nm, and $V_g = 1$ V.

3.2. Impact of Different Cavity Thickness in DM-LTFET

From the results of the previous section, we know that when $k = 23$, the DM-LTFET sensor had the strongest sensitivity. Therefore, in order to study the effect of different cavity thicknesses on the proposed sensor characteristics more clearly, this section discusses the results of the DM-LTFET being studied under the condition of $k = 23$.

Figure 4 illustrates that with an increase in the cavity thicknesses (T_c), the transfer curve of the device moved to the lower-right corner and the I_{on} and I_{on}/I_{off} sensitivity of the DM-LTFET sensor became smaller. As T_c increased, the actual gate oxide thickness under the gate electrode increased. When the same gate voltage was applied, the energy band of the body region of the device with a smaller T_c bent more severely such that the tunneling current and the current collected by the drain electrode was larger. However, the drain current under off-state conditions did not change much. Therefore, as T_c increased, the I_{on}/I_{off} also decreased. Figure 5 depicts that as T_c increased, the device became more and more difficult to turn on, and the threshold voltage also increased.

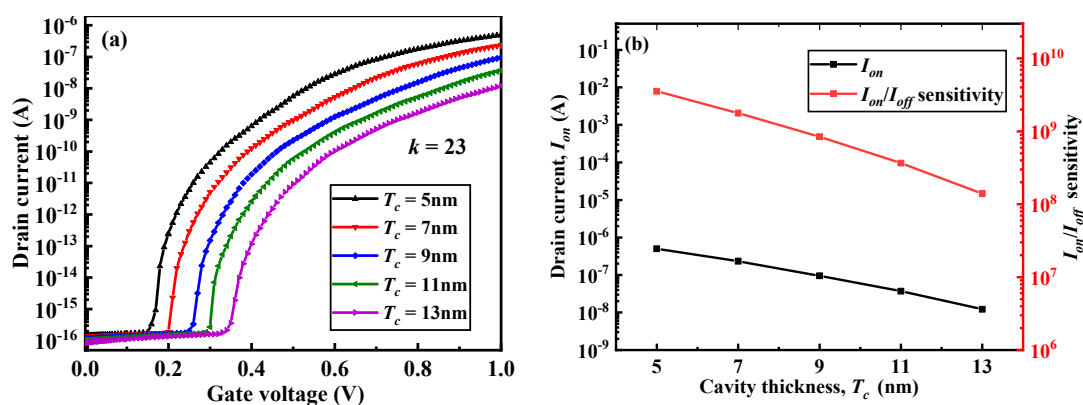


Figure 4. (a) Transfer characteristics and (b) I_{on} and I_{on}/I_{off} sensitivity of the DM-LTFET biosensor for different values of the cavity thickness (T_c) at $V_d = 0.5$ V, $V_g = 1$ V, and $k = 23$.

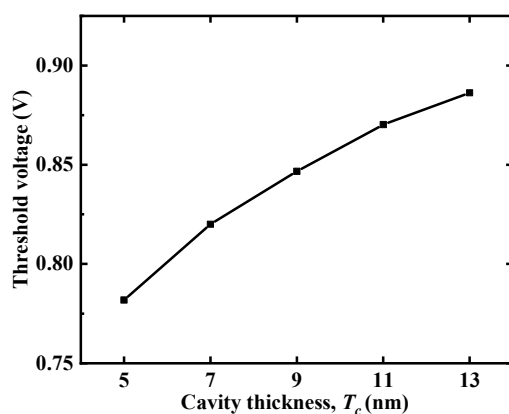


Figure 5. Threshold voltage of the DM-LTFET at $V_g = 1$ V, $V_d = 0.5$ V, and $k = 23$.

3.3. Impact of Charged Biomolecules on the DM-LTFET

The biomolecules that filled the cavity in the previous sections were uncharged; therefore, this section mainly discusses the effects of the differently charged biomolecules on the DM-LTFET sensor. In this study, the DM-LTFET biosensor detected the charged concentration of sensitive materials in the range of 10^{10} – 10^{13} cm^{-2} , which is a wide detection range compared with other sensors [25].

Figure 6 shows the transfer curves of biomolecules with different k values when the charge amount was different. When the biomolecules were positively charged, the transfer curve shifted to the left as the amount of charge increased. However, when the

biomolecules were negatively charged, as the amount of charge increased, the transfer curve shifted to the right. Moreover, as the value of k increased, the transfer curve also shifted to the left, which was consistent with the results in the previous section.

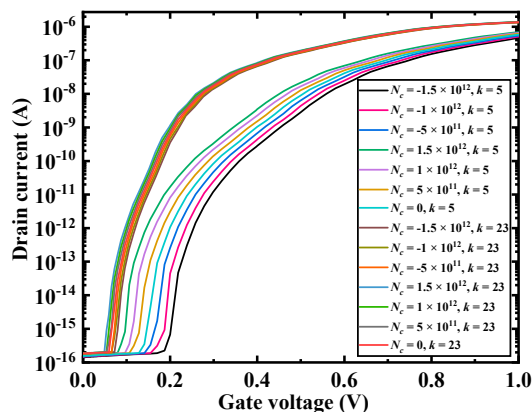


Figure 6. Transfer characteristics of the DM-LTFET biosensor for different dielectric constants and biomolecules charges at $V_d = 0.5$ V, $V_g = 1$ V, and $T_c = 5$ nm.

Figure 7 depicts the influence of different positive charges of different biomolecules on S_{cur} , V_{th} , and S_{Vth} . It can be seen from Figure 7a that for a given value of k , with an increase in the charge of the biomolecules, S_{cur} slowly increased. Figure 7b shows that as the amount of positive charge increased, the V_{th} of the device slowly decreased, and S_{Vth} slowly increased. As the amount of positive charge increased, the equivalent gate voltage applied to the gate increased, and the DM-LTFET was more likely to be turned on; therefore, V_{th} decreased and I_{on} increased. This further increased S_{cur} and S_{Vth} .

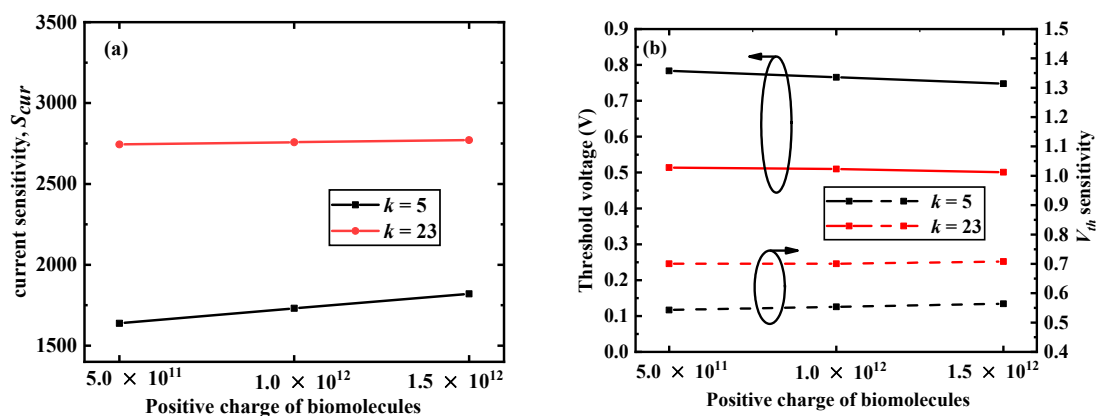


Figure 7. (a) Effect of different positive charges of the biomolecules on the current sensitivity and (b) V_{th} and S_{Vth} of the DM-LTFET at $V_g = 1$ V, $V_d = 0.5$ V, $k = 2.5$ and 23 , and $T_c = 5$ nm.

In Figure 8, the difference from the positively charged case was that at a given value of k , with more negative charges, S_{cur} slowly decreased and S_{Vth} also slowly decreased. At the same time, V_{th} increased. As the amount of negative charge increased, the equivalent gate voltage applied to the gate decreased and it was harder to turn on the DM-LTFET; therefore, V_{th} increased and I_{on} decreased. This further decreased S_{cur} and S_{Vth} .

In general, as the amount of the charge of the biomolecules changed, the sensitivity of the device also changed slightly, which was much smaller than the change in sensitivity caused by changing the k value of the biomolecules.

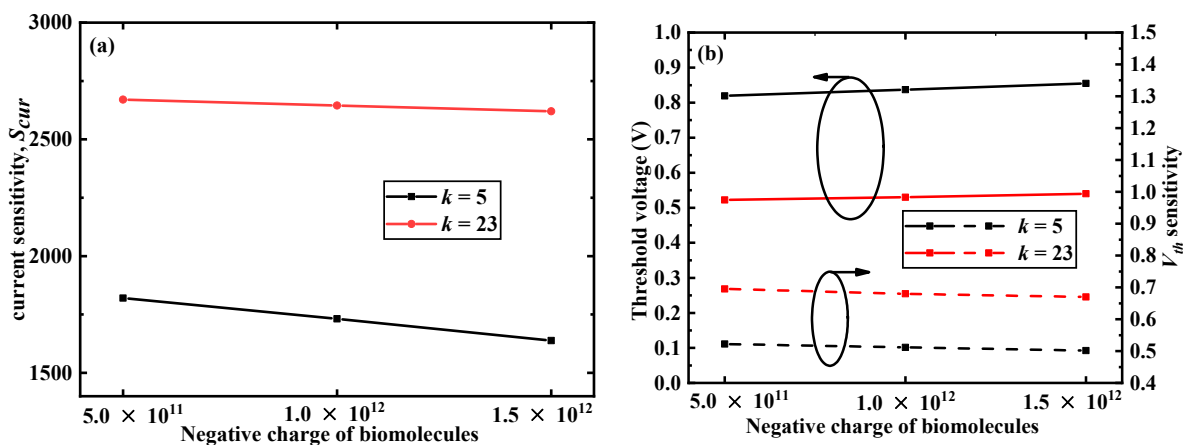


Figure 8. (a) Effect of different negative charge of biomolecules on current sensitivity and (b) V_{th} and $S_{V_{th}}$ of the DM-LTFET at $V_g = 1$ V, $V_d = 0.5$ V, $k = 5$ and 23, and $T_c = 5$ nm.

3.4. Comparison with the Biosensor-Based TFET

In Figure 9a,b, we show the comparison of the DM-LTFET metrics with previously published papers. It can be clearly seen from Figure 9a that, compared with previously published papers [16–18,20,26] (which have double gates), the DM-LTFET could simultaneously have a larger on-state current and I_{on}/I_{off} sensitivity. At the same time, it can be obviously seen from Figure 9b that the current sensitivity and sub-threshold swing sensitivity of the proposed structure were higher than those of the past published papers [16,18–20].

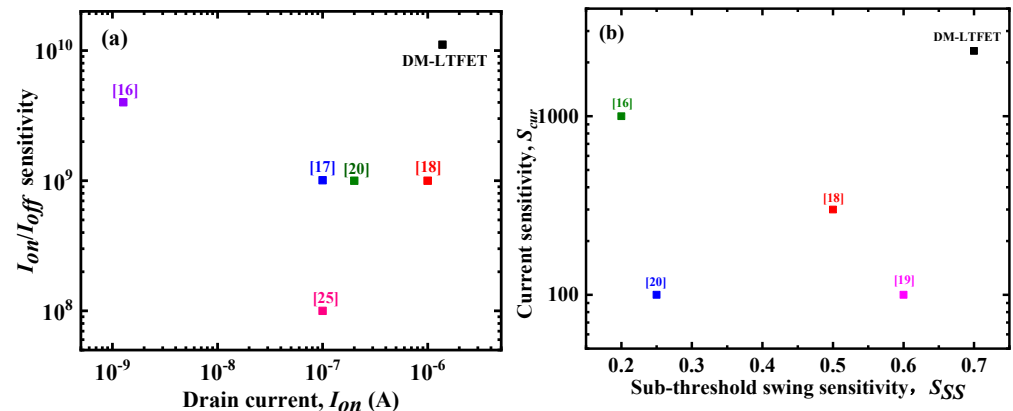


Figure 9. Comparison of the I_{on}/I_{off} sensitivity and current sensitivity of the DM-LTFET sensor with the other TFET based sensors in terms of (a) the on-state current and (b) the sub-threshold swing sensitivity.

4. Conclusions

In conclusion, the sensitivity of the DM-LTFET sensor was relatively high, which is very suitable for applications in the field of ultra-sensitive, low-consumption biosensors. The sensitivity of the DM-LTFET sensor was mainly investigated by studying the transfer curve, current sensitivity, and threshold voltage sensitivity of the proposed structure with different dielectric constants, cavity thicknesses, and charged biomolecules. It can be seen from the simulation results that the greater the relative permittivity of the biomolecules, the smaller the cavity, the greater the amount of positive charge, and the higher the sensitivity of the proposed sensor. Therefore, DM-LTFET sensors have profound development potential and market prospects.

Author Contributions: Conceptualization and writing—original draft preparation, C.C.; methodology, S.W. and S.C.; validation, C.C. and H.X.; writing—review and editing, H.L. and S.W.; funding acquisition, H.L. All authors have read and agreed to the published version of the manuscript.

Funding: This research was funded by the National Natural Science Foundation of China (grant no. U1866212), the Laboratory Open Fund of Beijing Smart-Chip Microelectronics Technology Co., Ltd. (grant no. SGITZXDDKJQT2002303), and the Innovation Foundation of Radiation Application (grant no. KFZC2018040206).

Conflicts of Interest: The authors declare no conflict of interest.

References

- Lee, C.-T.; Chiu, Y.-S.; Lou, L.-R.; Ho, S.-C.; Chuang, C.-T. Integrated pH sensors and performance improvement mechanism of ZnO-based ion-sensitive field-effect transistors. *IEEE Sens. J.* **2014**, *14*, 490–496. [\[CrossRef\]](#)
- Kwon, D.; Lee, J.H.; Kim, S.; Lee, R.; Mo, H.; Park, J.; Kim, D.H.; Park, B.-G. Drift-free pH detection with silicon nanowire field-effect transistors. *IEEE Electron Device Lett.* **2016**, *37*, 652–655. [\[CrossRef\]](#)
- Tamersit, K.; Djeflal, F. Double-gate graphene nanoribbon field-effect transistor for Dna and gas sensing applications: Simulation study and sensitivity analysis. *IEEE Sens. J.* **2016**, *16*, 4180–4191. [\[CrossRef\]](#)
- Wu, M.; Shin, J.; Hong, T.; Jin, X.; Lee, J.-H. Pulse biasing scheme for the fast recovery of FET-Type gas sensors for reducing gases. *IEEE Electron Device Lett.* **2017**, *38*, 971–974. [\[CrossRef\]](#)
- Song, Z.; Tang, Q.; Tong, Y.; Liu, Y. High-response identifiable gas sensor based on a gas-dielectric ZnPc nanobelt FET. *IEEE Electr. Device Lett.* **2017**, *38*, 1586–1589. [\[CrossRef\]](#)
- Lu, H.; Seabaugh, A. Tunnel field-effect transistors: State-of-the-art. *IEEE J. Electron Devices Soc.* **2014**, *2*, 44–49. [\[CrossRef\]](#)
- Li, W.; Liu, H.; Wang, S.; Chen, S.; Yang, Z. Design of high performance Si/SiGe heterojunction tunneling FETs with a T-shaped gate. *Nanoscale Res. Lett.* **2017**, *12*, 4–11. [\[CrossRef\]](#)
- Chen, S.; Wang, S.; Liu, H.; Li, W.; Wang, Q.; Wang, X. Symmetric U-shaped gate tunnel field-effect transistor. *IEEE Trans. Electron Devices* **2017**, *64*, 1343–1349. [\[CrossRef\]](#)
- Beniwal, S.; Saini, G. L-shaped tunneling field effect transistor with hetero-gate dielectric and hetero dielectric box. In Proceedings of the 2019 3rd International Conference on Trends in Electronics and Informatics (ICOEI), Tirunelveli, India, 23–25 April 2019.
- Zhu, J.; Zhao, Y.; Huang, Q. Design and simulation of a novel graded-channel heterojunction tunnel FET with high ION/I OFF ratio and steep swing. *IEEE Electr. Device Lett.* **2017**, *38*, 1200–1203. [\[CrossRef\]](#)
- Anand, S.; Singh, S.A.; Amin, I.; Asmita, S.T. Design and performance analysis of dielectrically modulated doping-less tunnel FET-based label free biosensor. *IEEE Sens. J.* **2019**, *19*, 4369–4374. [\[CrossRef\]](#)
- Tamersit, K.; Djeflal, F. Carbon nanotube field-effect transistor with vacuum gate dielectric for label-free detection of DNA molecules: A computational investigation. *IEEE Sens. J.* **2019**, *19*, 9263–9270. [\[CrossRef\]](#)
- Singh, A.D.; Sinha, S. Design and simulation of silicon-on-insulator based dielectric-modulated field effect transistor for biosensing applications. In Proceedings of the 2019 3rd International Conference on Electronics, Materials Engineering and Nano-Technology, Kolkata, India, 29–31 August 2019.
- Yadav, S.; Gedam, A.; Tirkey, S. A dielectric modulated biosensor for SARS-CoV-2. *IEEE Sens. J.* **2020**. [\[CrossRef\]](#)
- Wadhwa, G.; Raj, B. Parametric variation analysis of symmetric double gate charge plasma JLTFET for biosensor application. *IEEE Sens. J.* **2018**, *18*, 6070–6077. [\[CrossRef\]](#)
- Singh, D.; Pandey, S.; Nigam, K.; Sharma, D.; Singh, Y.D.; Kondekar, P. A charge-plasma-based dielectric-modulated junctionless TFET for biosensor label-free detection. *IEEE Trans. Electron Devices* **2017**, *64*, 271–278. [\[CrossRef\]](#)
- Verma, M.; Tirkey, S.; Yadav, S.; Sharma, D.; Singh, Y.D. Performance assessment of a novel vertical dielectrically modulated TFET-based biosensor. *IEEE Trans. Electron Devices* **2017**, *64*, 3841–3848. [\[CrossRef\]](#)
- Dwivedi, P.; Singh, R. Investigation the impact of the gate work-function and biases on the sensing metrics of TFET based biosensors. *Eng. Res. Expr.* **2020**, *20*, 10405–10414. [\[CrossRef\]](#)
- Kanungo, S.; Chattopadhyay, S.; Gupta, P.S.; Sinha, K.; Rahaman, H. Study and analysis of the effects of SiGe source and pocket-doped channel on sensing performance of dielectrically modulated tunnel FET-based biosensors. *IEEE Trans. Electron Devices* **2016**, *63*, 2589–2596. [\[CrossRef\]](#)
- Wadhwa, G.; Raj, B. Design, simulation and performance analysis of JLTFET biosensor for high sensitivity. *IEEE Trans. Nanotechnol.* **2018**, *18*, 567–574. [\[CrossRef\]](#)
- Mohammad, K.; Zeinab, A.; Ramezani, I.S.; Tamersit, A.K.; Mahdavi, N.A. Profound analysis on sensing performance of Nanogap SiGe source DM-TFET biosensor. *J. Mater. Sci. Mater. Electron.* **2020**. [\[CrossRef\]](#)
- Wadhwa, G.; Kamboj, P.; Raj, B. Design optimisation of junctionless TFET biosensor for high sensitivity. *Adv. Nat. Sci. Nanosci. Nanotechnol.* **2019**, *10*, 045001. [\[CrossRef\]](#)
- Kumar, S.; Singh, T.; Singh, B.; Tiwari, P.K. Simulation study of dielectric modulated dual channel trench gate TFET based biosensor. *IEEE Sens. J.* **2020**. [\[CrossRef\]](#)
- Wang, Q.; Liu, H.; Wang, S.; Chen, S. TCAD simulation of single-event-transient effects in L-shaped channel tunneling field-effect transistors. *IEEE Trans. Nucl. Sci.* **2018**, *65*, 2250–2259. [\[CrossRef\]](#)

-
25. Moon, D.-I.; Han, J.-W.; Meyyappan, M. Comparative study of field effect transistor based biosensors. *IEEE Trans. Nanotechnol.* **2016**, *15*, 956–961. [[CrossRef](#)]
 26. Kanungo, S.; Chattopadhyay, S.; Gupta, P.S.; Rahaman, H. Comparative performance analysis of the dielectrically modulated full-gate and short-gate tunnel FET-based biosensors. *IEEE Trans. Electron Devices* **2015**, *14*, 427–435. [[CrossRef](#)]